

# High-pressure stability, transformations, and vibrational dynamics of nitrosonium nitrate from synchrotron infrared and Raman spectroscopy

Yang Song<sup>a)</sup>

*Department of Chemistry and Chemical Biology, Harvard University, Cambridge, Massachusetts 02138 and Geophysical Laboratory, Carnegie Institution of Washington, Washington, D.C. 20015*

Russell J. Hemley, Zhenxian Liu, Maddury Somayazulu, and Ho-kwang Mao  
*Geophysical Laboratory, Carnegie Institution of Washington, Washington, D.C. 20015*

Dudley R. Herschbach

*Department of Chemistry and Chemical Biology, Harvard University, Cambridge, Massachusetts 02138*

(Received 20 December 2002; accepted 5 May 2003)

The properties of nitrosonium nitrate ( $\text{NO}^+\text{NO}_3^-$ ) were investigated following synthesis by laser heating of  $\text{N}_2\text{O}$  and  $\text{N}_2\text{O}_4$  under high pressures in a diamond anvil cell. Synchrotron infrared absorption spectra of  $\text{NO}^+\text{NO}_3^-$  were measured at pressures up to 32 GPa at room temperature. Raman spectra were obtained at pressures up to 40 GPa at room temperature and up to 14 GPa at temperatures down to 80 K. For both lattice and intramolecular vibrational modes, a smooth evolution of spectral bands with pressure indicates that  $\text{NO}^+\text{NO}_3^-$  forms a single phase over a broad range above 10 GPa, whereas marked changes, particularly evident in the Raman spectra at low temperature, indicate a phase transition occurs near 5 GPa.  $\text{NO}^+\text{NO}_3^-$  could be recovered at atmospheric pressure and low temperature, persisting to 180 K. The Raman and IR spectroscopic data suggest that the  $\text{NO}^+\text{NO}_3^-$  produced by laser heating of  $\text{N}_2\text{O}$  followed by decompression may differ in structure or orientational order-disorder from that produced by autoionization of  $\text{N}_2\text{O}_4$ .

© 2003 American Institute of Physics. [DOI: 10.1063/1.1586695]

## I. INTRODUCTION

Recent developments in diamond anvil cell techniques have opened new avenues for exploring the behavior of simple molecules at high densities.<sup>1</sup> At high pressures, many molecular systems exhibit extraordinary properties, phase transitions, or chemical reactions. Of these systems, nitrogen oxides have received particular attention as important species involved in combustion and in the storage of chemical energy. Moreover, instead of the simple pressure-induced polymerization observed in numerous systems, these compounds undergo intriguing and still poorly understood chemical transformations in condensed phase.<sup>2</sup> For instance, solid nitric oxide (NO) disproportionates into nitrous oxide ( $\text{N}_2\text{O}$ ) and dinitrogen tetroxide ( $\text{N}_2\text{O}_4$ ) at 176 K and 1.5 GPa.<sup>3</sup> The latter readily undergoes a subsequent transformation to a remarkable stable ionic isomer, nitrosonium nitrate ( $\text{NO}^+\text{NO}_3^-$ ). This ionic species and its molecular precursor,  $\text{N}_2\text{O}_4$ , have been the subject of several previous studies.<sup>4-9</sup> However, the mechanism governing the transformation between the two forms remain unclear. The formation of  $\text{NO}^+\text{NO}_3^-$  was first detected by Parts and Miller<sup>4</sup> in IR spectra of oxidized NO. Subsequent experiments on  $\text{N}_2\text{O}_4$  by Bolduan and Jodl<sup>5</sup> established that the ionic form could be spontaneously produced when  $\text{N}_2\text{O}_4$  is trapped in a Ne matrix. Later, the same group obtained Raman spectra of solid  $\text{N}_2\text{O}_4$  and observed the formation of ionic  $\text{NO}^+\text{NO}_3^-$  by

temperature-induced autoionization of  $\text{N}_2\text{O}_4$ .<sup>6</sup> In these ambient pressure studies, the formation of the ionic nitrosonium nitrate species was observed only in the amorphous solid and only at temperatures below 180 K; its formation was attributed to an intermediate asymmetric ONONO<sub>2</sub> isomer (designated D' in Ref. 6) or to photolysis of  $\text{NO}_2$  monomers.

The transformation of molecular  $\text{N}_2\text{O}_4$  to ionic  $\text{NO}^+\text{NO}_3^-$  under high pressures was first observed by Jones and co-workers.<sup>7,8</sup> They discovered that laser irradiation of cubic *Im3*  $\alpha$ - $\text{N}_2\text{O}_4$  results in the formation of  $\beta$ - $\text{N}_2\text{O}_4$  with unknown noncubic structure at 1.16 GPa at room temperature. Under pressures of 1.5–3.0 GPa at room temperature,  $\beta$ - $\text{N}_2\text{O}_4$  exhibits a reversible phase transition to the ionic form of  $\text{NO}^+\text{NO}_3^-$  with a large hysteresis. Recently, Somayazulu *et al.*<sup>9</sup> found a different way to synthesize  $\text{NO}^+\text{NO}_3^-$  under pressure. At 10–30 GPa laser heating to 1000–2000 K transforms  $\text{N}_2\text{O}$  via the reaction  $4\text{N}_2\text{O} \rightarrow \text{NO}^+\text{NO}_3^- + 3\text{N}_2$ . Angular dispersive x-ray diffraction patterns of the products indicated an orthorhombic structure for  $\text{NO}^+\text{NO}_3^-$  at high pressures. Subsequent x-ray diffraction measurements<sup>10</sup> have provided further information about  $\text{NO}^+\text{NO}_3^-$ , including the pressure-volume equation of state.

Complete characterization of  $\text{NO}^+\text{NO}_3^-$  requires detailed study by IR and Raman spectroscopy under a variety of conditions. Here we report such data for both the far and mid-IR regions for  $\text{NO}^+\text{NO}_3^-$  at pressures up to 32 GPa. The far-IR measurements appear to be the first absorption data at low wave numbers at any pressure for this compound. Ra-

<sup>a)</sup> Author to whom all correspondence should be addressed. Electronic mail: ysong@chemistry.harvard.edu

TABLE I. Observed IR and Raman frequencies for  $\text{NO}^+\text{NO}_3^-$  (and transformed species) and assignments at various pressures and temperatures.

IR ( $\text{cm}^{-1}$ ) <sup>a</sup>			Raman ( $\text{cm}^{-1}$ ) <sup>b</sup>				Assignment
32 GPa	0.6 GPa	Ref. <sup>c</sup>	80 K	190 K	Ref. <sup>d</sup>	Ref. <sup>e</sup>	
	167		50,87,117,	71	62(s),		Lattice modes
372			132,150,	118	124(w)		Lattice modes
659	431,532,589		173,221,258				Lattice modes
				278		282.8	$\nu_3$ ( $A_g$ ) N–N str
				495		498.2	$\nu_6$ ( $B_{1g}$ ) $\text{NO}_2$ rock
				639		639	$\nu_6$ ( $A'$ ) O=N–O bend
				678		676.8	$\nu_8$ ( $B_{1g}$ ) $\text{NO}_2$ wag
	743	747					$\nu_{12}$ ( $B_{3u}$ , $\text{NO}_2$ def)
762			716		714(w)		$\nu_4$ ( $E'$ , $\text{NO}_3^-$ in-plane def)
				814		811.7	$\nu_2$ ( $A_g$ ) $\text{NO}_2$ sym bend
836		813	823				$\nu_2$ ( $A_2''$ , $\text{NO}_3^-$ out-plane bend)
1034							lattice combinations
1133		1014	1049		1045(s)		$\nu_1$ ( $A_1'$ , $\text{NO}_3^-$ sym str)
	1250	1248					$\nu_{11}$ ( $B_{3u}$ , $\text{NO}_2$ sym str)
				1382		1382.3	$\nu_1$ ( $A_g$ , $\text{NO}_2$ sym str)
1404	1385	1385			1330,1400(w)		$\nu_3$ ( $E'$ , $\text{NO}_3^-$ antisym str)
			1640				$2\nu_2$ ( $\text{NO}_3^-$ )
	1723	1722					$\nu_9$ ( $B_{2u}$ , $\text{NO}_2$ antisym str)
				1724		1723.5	$\nu_5$ ( $B_{1g}$ , $\text{NO}_2$ antisym str)
1738							$\nu_1 + \text{lattice}$ ( $\text{NO}_3^-$ )
1840							$\nu_1 + \nu_4$
2265		2292	2243	2237	2267(vs)		$\nu_{\text{NO}^+}$
2340	2232						?
2439	2353						$\nu_3 + \text{lattice modes}$

<sup>a</sup>Infrared bands measured at room temperature.

<sup>b</sup>Raman active modes measured at ambient pressure and 80 and 190 K.

<sup>c</sup>Reference 13, for atmospheric pressure and 20 K.

<sup>d</sup>Reference 15, for atmospheric pressure and low temperature.

<sup>e</sup>Reference 6, for atmospheric pressure and low temperature.

man spectra of  $\text{NO}^+\text{NO}_3^-$  were obtained at room temperature as well as temperatures down to 80 K and pressures up to 40 GPa. These optical spectra, especially the low-temperature Raman data, elucidate important aspects of the transformation, thermodynamic properties, and structure of  $\text{NO}^+\text{NO}_3^-$ .

## II. EXPERIMENTAL PROCEDURES

Pure  $\text{N}_2\text{O}$  (99%) and  $\text{N}_2\text{O}_4$  (99.5%) gas was purchased from Aldrich and used without further purification. Loading was done by precooling a diamond anvil cell in liquid nitrogen. The melting point for  $\text{N}_2\text{O}$  is  $-90^\circ\text{C}$  so gaseous  $\text{N}_2\text{O}$  solidifies on the cooled rhenium gasket of the cell in a liquid nitrogen bath. The cells were then sealed and the solid  $\text{N}_2\text{O}$  pressurized before warming up to room temperature. The pressure was determined from the pressure shift of the  $R_1$  ruby fluorescence line, according to the relationship<sup>11</sup>

$$P(\text{GPa}) = A/B[\{1 + \Delta\lambda(T)/\lambda_0(T)\}^B - 1], \quad (1)$$

where  $A = 1904$  GPa,  $B = 7.665$ ,  $\lambda_0(T) = 694.28$  nm at 298 K and  $\Delta\lambda(T)$  is the difference between the wavelength of the  $R_1$  line at pressure  $P$  and that at atmospheric pressure. The accuracy of the pressure measurement was  $\pm 0.05$  GPa under quasi-hydrostatic conditions.

Samples were heated by a  $\text{CO}_2$  infrared laser (10.6  $\mu\text{m}$  lines) operated at about 50 W typically at 15 GPa. The laser beam was focused to less than 30  $\mu\text{m}$  to achieve an estimated temperature of 1000–2000 K. The transformation of  $\text{N}_2\text{O}$  to  $\text{NO}^+\text{NO}_3^-$  was instantaneous at high temperature and

irreversible when the sample was quenched to room temperature at high pressures ( $>10$  GPa). The completion of transformation was confirmed by Raman spectroscopy.

Infrared absorption measurements were performed at beamline U2A at the National Synchrotron Light Source of Brookhaven National Laboratory. The optical layout of the setup has been described in detail previously.<sup>12</sup> Briefly, the synchrotron light is collected from a source in a  $40 \times 40$  mrad solid angle and collimated to a 1.5-in.-diam beam before entering a Bruker IFS 66V vacuum FT spectrometer. The spectrometer is equipped with a number of beam splitters and detectors including a silicon bolometer and MCT. In addition, a grating spectrograph with a CCD array detector is used in the visible, giving complete coverage of the spectral range from 50 to 2000  $\text{cm}^{-1}$ . The resolution used in the present study is 4  $\text{cm}^{-1}$ .

Raman spectroscopy was performed at the Geophysical Laboratory. Both the 488.0 and 514.5 nm lines of a Coherent Innova  $\text{Ar}^+$  laser were used as the excitation source, with average power of 0.4 W for the spectral measurements. The collimated laser beam was typically focused on the sample in a backscattering geometry with an estimated power of less than 100 mW. The resolution achieved using a 460 mm focal length  $f/5.3$  imaging spectrograph (ISA HR460) equipped with an 1800 grooves/mm grating was  $\pm 0.1$   $\text{cm}^{-1}$ . The calibration of the Raman scattering was done using Ne lines with an uncertainty of  $\pm 1$   $\text{cm}^{-1}$ . For the low-temperature Raman measurements, an optical cryostat was used; the tem-

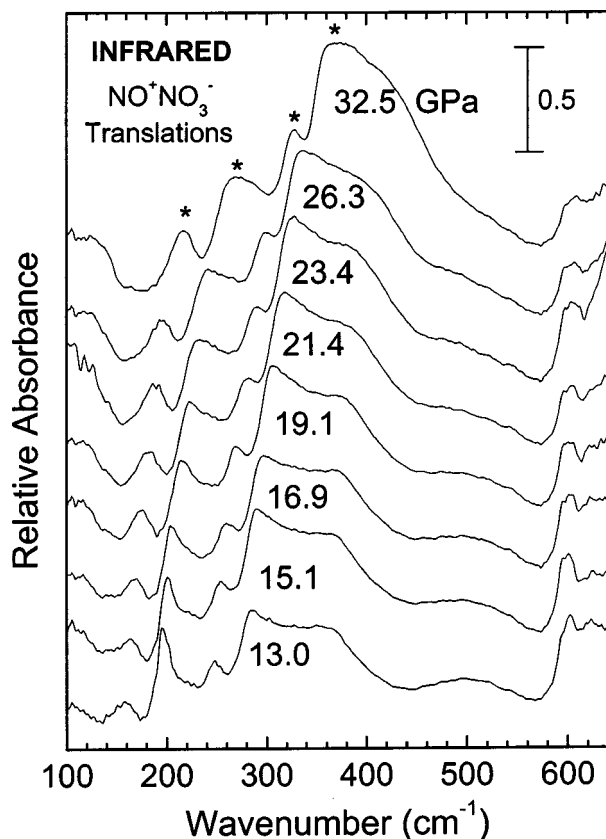


FIG. 1. Far-IR spectra of  $\text{NO}^+\text{NO}_3^-$  in the range  $100\text{--}600\text{ cm}^{-1}$  measured at room temperature for eight pressures (labeled in GPa). At each pressure, the absorbance has been normalized to adjust for changes in the beam current of the synchrotron light source. The asterisks (\*) denote the translational modes (see the text).

perature range from 80 to 300 K was explored using liquid nitrogen as the cryogen.

### III. RESULTS

Table I lists vibrational frequencies assigned to  $\text{NO}^+\text{NO}_3^-$  and related species; the IR data pertain to room temperature and pressures of 32 and 0.6 GPa, the Raman spectra to atmospheric pressure and temperatures of 80 or 190 K. Most of the data were obtained from laser heating  $\text{N}_2\text{O}$  under pressure, although the results for laser heated  $\text{N}_2\text{O}_4$  are also included. Where available, results from previous spectroscopic studies, at atmospheric pressure and low temperature, are included for comparison.

#### A. Far-IR spectra

Figure 1 shows far-infrared absorption spectra of  $\text{NO}^+\text{NO}_3^-$  in the region  $100\text{--}600\text{ cm}^{-1}$  collected at room temperature and eight selected pressures. Due to the small sample size (diameter about  $150\text{ }\mu\text{m}$ ) the diffraction limit was near  $100\text{ cm}^{-1}$  and thus absorption bands below that could not be observed unambiguously. The major feature in the far-IR is a broad band, peaking at  $372\text{ cm}^{-1}$  at 32.5 GPa, with several shoulders at lower frequencies. This peak and the shoulders can be assigned to lattice modes of  $\text{NO}^+\text{NO}_3^-$ . The absorption intensity of the major lattice mode decreases with decreasing pressure. This trend resembles the IR activ-

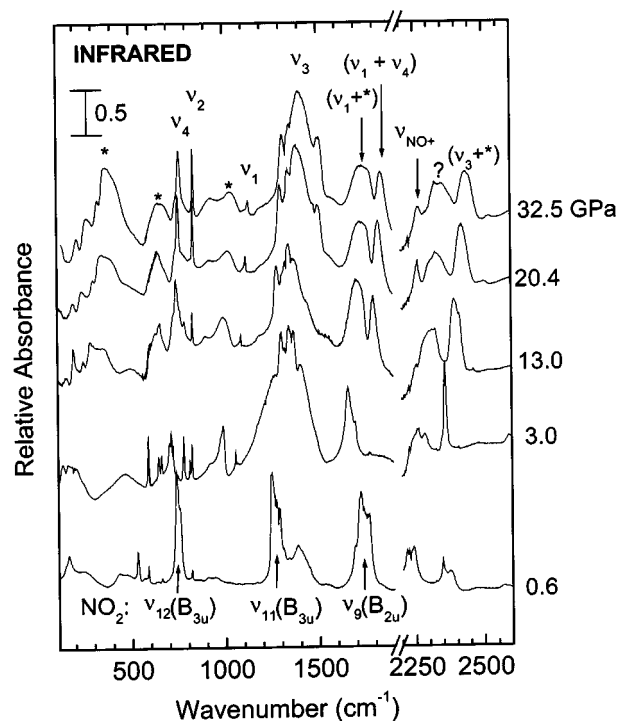


FIG. 2. IR spectra of  $\text{NO}^+\text{NO}_3^-$  in the range  $100\text{--}2500\text{ cm}^{-1}$  measured at room temperature for five pressures (indicated in GPa on the right-hand ordinate). The absorbance has been normalized with respect to the beam current of the synchrotron light source. The sample thickness was about  $23\text{ }\mu\text{m}$ . The region  $1900\text{--}2200\text{ cm}^{-1}$  is omitted because of interfering absorptions from the type II diamonds used as anvils. Asterisks (\*) indicate lattice modes or combinations.

ity previously seen in the mid-IR region,<sup>9</sup> indicating that the ionic character of  $\text{NO}^+\text{NO}_3^-$  increases with compression. However, the far-IR lattice mode had not been observed previously, either in IR spectra of  $\text{N}_2\text{O}_4$  at atmospheric pressure<sup>13–15</sup> or in  $\text{NO}^+\text{NO}_3^-$  at high pressure.<sup>9</sup> As the pressure was decreased from 32.5 to 9.5 GPa, the positions of the lattice modes shift smoothly and gradually downwards. This indicates the existence of only one phase in this pressure region, consistent with our x-ray diffraction measurements.<sup>10</sup>

#### B. Mid-IR spectra

Figure 2 shows the mid-IR spectra of  $\text{NO}^+\text{NO}_3^-$  obtained at room temperature and pressures ranging from 32.5 to 0.6 GPa. The region  $1900\text{--}2200\text{ cm}^{-1}$  is omitted because of interference by strong absorption from the type II diamonds used in the pressure cell. Above  $2500\text{ cm}^{-1}$ , no prominent absorption peaks were observed. At the highest pressure, 32.5 GPa, 12 IR bands are clearly resolved, as listed in Table I. Like the peak at  $372\text{ cm}^{-1}$  observed in the far-IR region, that centered at  $659\text{ cm}^{-1}$  is attributed to a lattice mode. The peaks observed at  $761$ ,  $836$ , and  $1133\text{ cm}^{-1}$  are assigned to vibrational modes of the  $\text{NO}_3^-$  anion, respectively  $\nu_4$  ( $E'$ , in plane bend),  $\nu_2$  ( $A_2''$ , out of plane bend) and  $\nu_1$  ( $A_1'$ , symmetric stretch). The assignment of  $\nu_4$  and  $\nu_2$  and their intensity enhancement at high pressure are consistent with our previous study of  $\text{NO}^+\text{NO}_3^-$  at high pressure,<sup>9</sup> but in that study the  $\nu_1$  mode was not observed. In previous atmospheric pressure studies<sup>13–16</sup> of  $\text{NO}^+\text{NO}_3^-$ , the

$\nu_4$ ,  $\nu_2$ , and  $\nu_1$  modes were all found to be very weak. The low intensity of the  $\nu_1$  band at all pressures indicates that the relatively small transition dipole moment of this symmetric stretch vibrational mode changes little with compression. Our observation of the  $\nu_4$ ,  $\nu_2$ , and  $\nu_1$  modes at all pressures above 1 GPa at room temperature provides a definitive identification of the  $\text{NO}_3^-$  anion; as described later, we also saw these three modes in the Raman spectra.

The peak centered at  $1034\text{ cm}^{-1}$  in Fig. 2 was not observed in the previous IR spectra of  $\text{NO}^+\text{NO}_3^-$ , either at high pressure<sup>9</sup> or atmospheric pressure.<sup>13–16</sup> As the pressure is reduced, it behaves much like the  $659\text{ cm}^{-1}$  band, as both become sharper and stronger. This suggests that the  $1034\text{ cm}^{-1}$  band is a combination of the two lattice modes at  $372$  and  $659\text{ cm}^{-1}$ . The intense and broad peak centered near  $1400\text{ cm}^{-1}$  is the most prominent feature in our IR spectra above 3 GPa. It could not be observed in the previous high pressure IR study<sup>9</sup> due to absorption by the type I diamonds used in that work.<sup>12</sup> This peak is assigned to  $\nu_3$ , the  $\text{NO}_3^-$  asymmetric stretching mode. Its high intensity is in accord with IR spectra of  $\text{NO}^+\text{NO}_3^-$  at atmospheric pressure,<sup>13–16</sup> and attributable to the large transition dipole associated with the antisymmetric stretching mode (in contrast to the symmetric  $\nu_1$  mode). Another diagnostic frequency for  $\text{NO}^+\text{NO}_3^-$  is the stretching mode of  $\text{NO}^+$ ; in Fig. 2, this appears near  $2265\text{ cm}^{-1}$  but could only be unambiguously observed at high pressures (32 and 20 GPa) because at lower pressures it is engulfed by a more intense absorption band (not yet assigned, as discussed in the following).

Four other strong peaks seen near  $1740$ ,  $1840$ ,  $2340$ ,  $2440\text{ cm}^{-1}$  at 32.5 GPa also appear consistently at lower pressures. The  $1840\text{ cm}^{-1}$  peak can be assigned to the ( $\nu_1 + \nu_4$ ) combination of  $\text{NO}^+\text{NO}_3^-$ . Accordingly, the  $1740\text{ cm}^{-1}$  band (suggested previously as  $\nu_1 + \nu_4$ )<sup>9</sup> could be associated with the combination of a far-IR lattice mode ( $372\text{ cm}^{-1}$ ) and the strong  $\nu_3$  band at  $1402\text{ cm}^{-1}$ . The peaks at  $2340$  and  $2440\text{ cm}^{-1}$ , which saturate due to strong absorption with thick samples,<sup>9</sup> are clearly resolved in Fig. 2, since a thinner ( $\sim 23\text{ }\mu\text{m}$ ) sample was employed here. These peaks seem likely to be combination bands but other possibilities are discussed in the following as well.

### C. Room-temperature Raman spectra

The Raman spectrum of  $\text{NO}^+\text{NO}_3^-$  was typically measured immediately after laser heating of  $\text{N}_2\text{O}$  to check the degree of completion of reaction and transformation. We found that from about 10 to 40 GPa, heating of  $\text{N}_2\text{O}$  results in an inhomogeneous mass within the cell that appears fabriclike to the eye. The presence of  $\text{NO}^+\text{NO}_3^-$  and  $\text{N}_2$  is confirmed by characteristic peaks (e.g., at 13 GPa) at  $740\text{ cm}^{-1}$  ( $\nu_4$ ),  $827\text{ cm}^{-1}$  ( $\nu_2$ ),  $1096\text{ cm}^{-1}$  ( $\nu_1$ ),  $2253\text{ cm}^{-1}$  ( $\nu_{\text{NO}^+}$ ),  $2362\text{ cm}^{-1}$ , and  $2383\text{ cm}^{-1}$  ( $\text{N}_2$ ) as well as abundant lattice modes below  $400\text{ cm}^{-1}$ . Figure 3 shows sample Raman spectra of  $\text{NO}^+\text{NO}_3^-$  obtained at five pressures ranging from 40.0 to 0.8 GPa. The major characteristic modes, (e.g.,  $\nu_4$ ,  $\nu_2$ ,  $\nu_1$ , and  $\nu_{\text{NO}^+}$ ) are seen to shift to lower frequencies on decreasing pressure. The Raman profiles of these internal vibrational modes typically change less with pressure than in

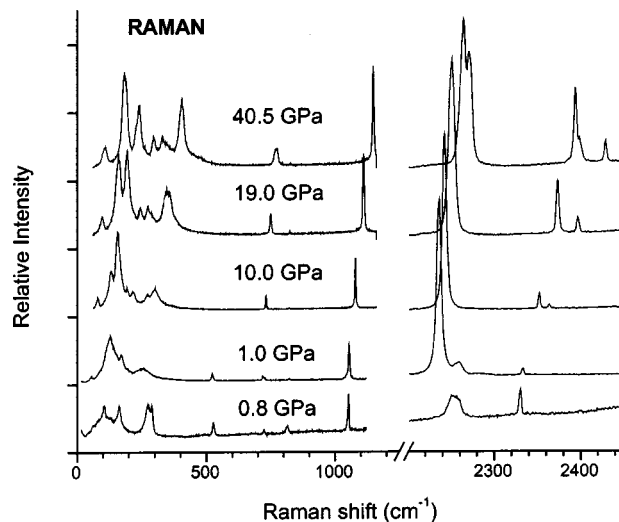


FIG. 3. Raman spectra of  $\text{NO}^+\text{NO}_3^-$  in the range  $50\text{--}2500\text{ cm}^{-1}$  measured at room temperature for five pressures (indicated in GPa).

the lattice region. Upon decompression, the number of resolvable Raman peaks is reduced as a result of peak broadening. This trend is consistent with the proposal<sup>9</sup> that  $\text{NO}^+\text{NO}_3^-$  becomes more disordered on decompression. When the pressure drops below 1 GPa, the Raman spectrum shows significant changes, in particular a broad peak near  $280\text{ cm}^{-1}$  is enhanced and the strong  $\text{NO}^+$  peak disappears. This accords with our low temperature results (discussed in the following), which suggest a phase transformation of  $\text{NO}^+\text{NO}_3^-$  occurs at low pressure.

On decompression from 40 to 1 GPa, changes in the room temperature Raman spectra appear to be steady and continuous. Accordingly, unlike the IR spectra, which exhibit changes in both the lattice and intramolecular modes indicative of a possible phase transition, the room-temperature Raman spectra show no major changes above 1 GPa. Moreover, the evolution of the peak positions with pressure is linear for  $\nu_4$ ,  $\nu_2$ ,  $\nu_1$ ,  $\nu_{\text{NO}^+}$  as well as the major lattice modes. Therefore, we undertook to obtain low-temperature Raman spectra in the expectation that peaks would be better resolved and thereby respond more sensitively to pressure.

### D. Raman spectra at low temperatures

Figure 4 displays the temperature dependence of the Raman shifts of  $\text{NO}^+\text{NO}_3^-$  at a nominal pressure near 14 GPa. During cooling from room temperature to 80 K, the pressure of the sample inside the cell increased slightly, causing the peaks to move to higher frequencies. With the temperature held constant at 80 K, the Raman spectra were measured as a function of pressure between 14 GPa and ambient. Selected spectra are plotted in Fig. 5. At such a low temperature, both the lattice and internal modes exhibit significant pressure shifts. For example, the peak centered at  $337\text{ cm}^{-1}$  at 14 GPa appears as a doublet at atmospheric pressure, with a separation of  $38\text{ cm}^{-1}$ . In addition, the two almost equally strong peaks centered at  $142$  and  $180\text{ cm}^{-1}$  evolve into a fairly weak peak at  $87\text{ cm}^{-1}$  and a much stronger peak at  $118\text{ cm}^{-1}$ , respectively. For the  $\nu_4$  mode near  $716\text{ cm}^{-1}$  a more



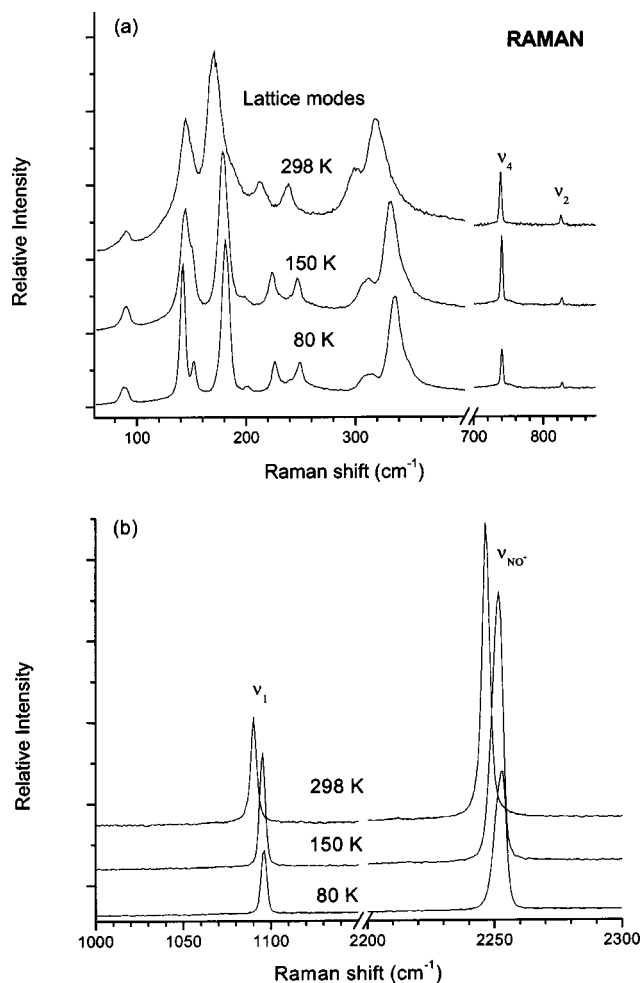


FIG. 4. Raman spectra of  $\text{NO}^+\text{NO}_3^-$  in the ranges (a) 60–900  $\text{cm}^{-1}$  and (b) 1000–2300  $\text{cm}^{-1}$  measured at constant nominal pressure of about 14 GPa at 298, 150, and 80 K.

striking change occurs; at high pressures, it is a singlet but as the pressure drops to 4.8 GPa and below, it develops into a doublet with a separation of 34  $\text{cm}^{-1}$ . We interpret these changes in the Raman spectrum as evidence for a phase transition in  $\text{NO}^+\text{NO}_3^-$ .

Figure 6 shows the variation of the peak positions of Raman modes in the lattice mode region observed at 80 K as a function of pressure. These bands exhibit a distinct change in  $(d\nu/dP)_T$  at about 5 GPa, indicating a transition occurs near that pressure. The behavior of the second highest frequency mode changes most markedly at 5 GPa. In addition, nine modes can be identified at high pressures while at low pressures (<5 GPa), only seven are discernible. The pressure dependence of higher frequency intramolecular modes (not shown) shows changes at 5 GPa, but this is much less pronounced. We note that the low-pressure phase remains at least partially ordered as indicated by the Raman features discussed in the following. The evolution of these Raman bands in the lattice-mode region was also examined on compression in a separate run. There are slight differences in slopes for several modes between compression and decompression (most likely due to different stress conditions), but a distinct change at 5 GPa on compression is still prominent,

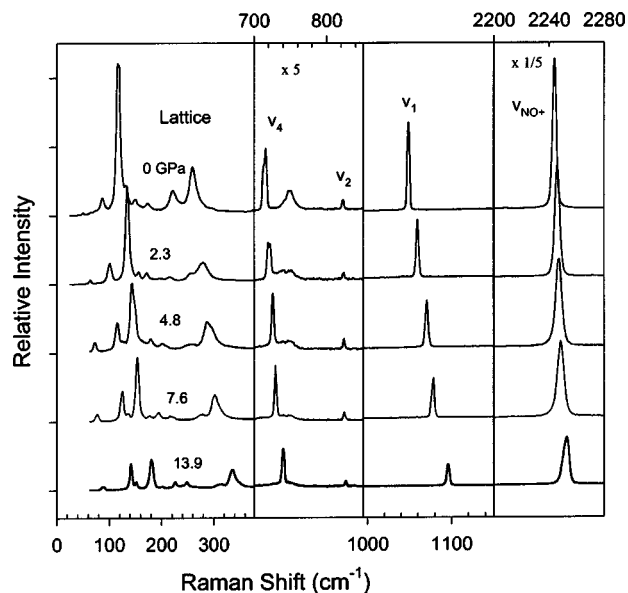


FIG. 5. Raman spectra of  $\text{NO}^+\text{NO}_3^-$  in the regions 50–380; 700–860; 1000–1150; and 2200–2280  $\text{cm}^{-1}$  measured near 80 K and five pressures. The measurements were performed at successive steps of decompression, starting from 13.9 GPa. Due to the low intensity of  $\nu_4$  and  $\nu_2$  and high intensity of  $\nu_{\text{NO}_3^-}$ , the spectra in the 700–850 and 2200–2280  $\text{cm}^{-1}$  regions are scaled by 5 and 1/5, respectively.

indicating the transition is reversible and has very little hysteresis.

Despite the presence of a transition, these low-temperature measurements also established that  $\text{NO}^+\text{NO}_3^-$  can be recovered at ambient pressure. We find that all the principal low- and high-frequency modes associated with  $\text{NO}^+\text{NO}_3^-$  persist down to ambient pressure. The accompanying  $\text{N}_2$  formed by the laser heating of  $\text{N}_2\text{O}$  has escaped, as

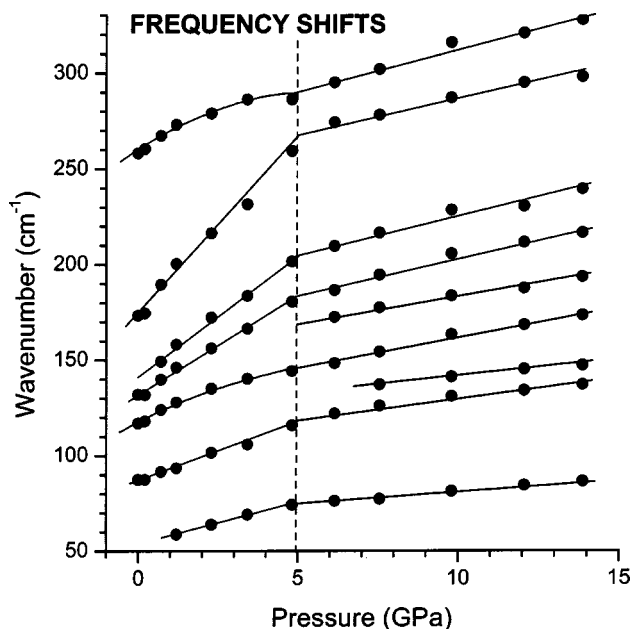


FIG. 6. Variation with pressure of Raman shifts in the lattice region (50–350  $\text{cm}^{-1}$ ) up to 15 GPa at 80 K. The lines are guides to the eye. The vertical dashed line at about 5 GPa indicates the approximate phase boundary.

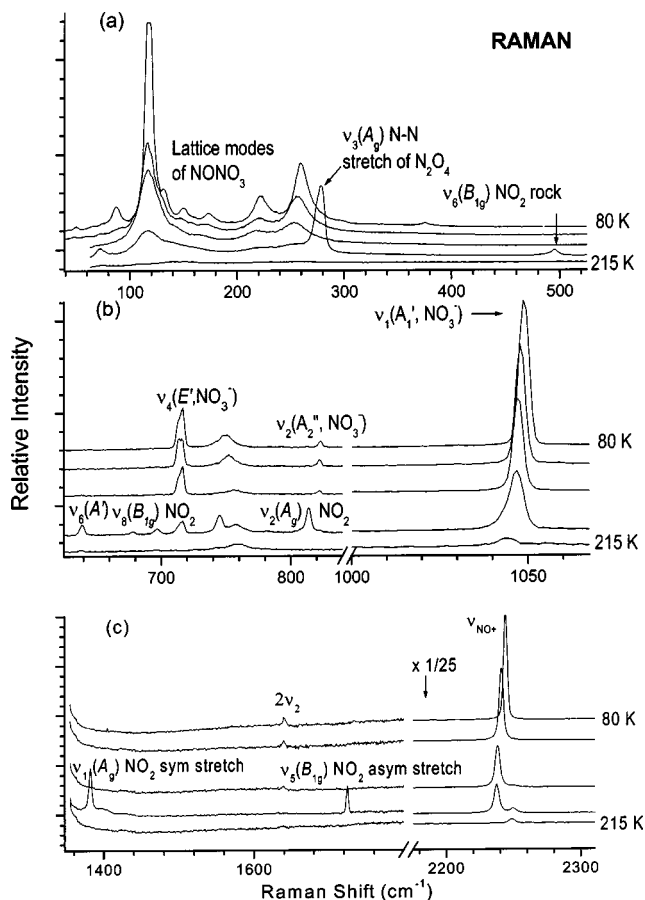


FIG. 7. Raman spectra of  $\text{NO}^+\text{NO}_3^-$  in the ranges of (a) 40–530  $\text{cm}^{-1}$ , (b) 630–1070  $\text{cm}^{-1}$  and (c) 1350–2300  $\text{cm}^{-1}$  measured at ambient pressure and five temperatures: 80, 135, 180, 190, and 215 K.

evidenced by the disappearance of the peaks at about 2350  $\text{cm}^{-1}$ , and  $\text{NO}^+\text{NO}_3^-$  appears to be the sole product. The sample was warmed at ambient pressure and Raman spectra of  $\text{NO}^+\text{NO}_3^-$  measured at five temperatures ranging from 80 to 215 K. Figure 7 gives a panoramic view of these spectra, for three regions. In the lattice mode region (a), peaks at 118, 222, and 260  $\text{cm}^{-1}$ , which are rather sharp at 80 K, become weaker and broader as the temperature increases from 80 to 180 K. While the peak at 118  $\text{cm}^{-1}$  has no obvious shift, the latter two exhibit noticeable shifts of  $-3$  and  $-6$   $\text{cm}^{-1}$ , respectively. In addition, the small peak at 87  $\text{cm}^{-1}$  disappears near 135 K. Other bands at 132, 150, and 174  $\text{cm}^{-1}$  also disappear when the temperature reaches 135 K. In the internal mode region (b) and (c), the frequencies of  $\nu_4$  and  $\nu_2$  are found to remain nearly constant with temperature, while  $\nu_1$  and  $\nu_{\text{NO}^+}$  modes exhibit a consistent shift to lower energy.

The highest temperature at which the  $\text{NO}^+\text{NO}_3^-$  retains its identity is found to be about 180 K. When the sample was heated to 190 K at ambient pressure, significant changes in the Raman spectrum were observed. The lattice mode region is reduced to two weak, broad peaks at 71 and 118  $\text{cm}^{-1}$ . In addition, a sharp and strong peak occurs at 278  $\text{cm}^{-1}$  that coincides with the  $\nu_3(A_g)$  N–N stretching mode of molecular  $\text{N}_2\text{O}_4$ . Other changes include the appearance of numerous Raman modes at 450–1800  $\text{cm}^{-1}$ , most of which can be assigned as internal modes associated with molecular  $\text{N}_2\text{O}_4$ ,

such as the  $\nu_6(B_{1g})$   $\text{NO}_2$  rocking mode at 495  $\text{cm}^{-1}$ , the  $\nu_6(A')$  O=N–O bend at 639  $\text{cm}^{-1}$ , the  $\nu_8(B_{1g})$   $\text{NO}_2$  wagging mode at 678  $\text{cm}^{-1}$ , the  $\nu_2(A_g)$   $\text{NO}_2$  symmetric bend at 814  $\text{cm}^{-1}$ , the  $\nu_1(A_g)$   $\text{NO}_2$  symmetric stretch at 1382  $\text{cm}^{-1}$  and the  $\nu_5(B_{1g})$   $\text{NO}_2$  antisymmetric stretch at 1724  $\text{cm}^{-1}$ .<sup>6,8,16</sup> However, the  $\nu_4$ ,  $\nu_1$ , and  $\nu_{\text{NO}^+}$  modes of  $\text{NO}^+\text{NO}_3^-$  still have discernible intensities. We conclude that at 190 K, ionic  $\text{NO}^+\text{NO}_3^-$  has mostly converted to molecular  $\text{N}_2\text{O}_4$  in bulk, so the Raman spectrum arises from a mixture of the two phases. Further heating of the sample to 215 K results in loss of sample due to evaporation and disappearance of the Raman features.

#### IV. DISCUSSION

The present work provides the first far-IR data at any pressure on this material, as well as a more complete study of the mid-IR and Raman spectra as a function of both pressure and temperature. Accurate assignments of the spectra require factor group analysis<sup>17</sup> based on detailed information on the crystal structures involved. X-ray diffraction studies<sup>9,10</sup> have provided determination of the unit-cell symmetry and constraints on possible space group, but no information on the atom coordinates needed for detailed symmetry assignments. Alternatively, we can compare the spectra with those of materials that appear related, such as  $\text{KNO}_3$ , whose IR and Raman spectra have been studied both experimentally and theoretically.<sup>18–20</sup> The legitimacy of this comparison relies on two facts: (a) the calculated topology of  $\text{NONO}_3$  exhibits a similar symmetry to the predicted stable bidentate geometry of  $\text{KNO}_3$ ,<sup>18</sup> both close to point group  $C_{2v}$ ; and (b) the stable phase of  $\text{KNO}_3$  at room temperature, phase II, also has an aragonite structure with four ion pairs per cell as does  $\text{NONO}_3$ .<sup>19,20</sup> The predicted ambient pressure IR-active modes involving the vibrations between the ion pairs of  $\text{KNO}_3$  ( $\text{NaNO}_3$ ) are  $\nu_4(A_1)$ : 234 (322)  $\text{cm}^{-1}$ ,  $\nu_9(B_2)$ : 187(255)  $\text{cm}^{-1}$  and  $\nu_6(B_1)$ : 73 (108)  $\text{cm}^{-1}$ .<sup>18</sup> There are 18 predicted active Raman modes in the lattice region of phase II  $\text{KNO}_3$ , as compared with fewer experimentally observed and reported in the region of 53–165  $\text{cm}^{-1}$ . Of these Raman modes, those below 100  $\text{cm}^{-1}$  are believed to be rotational (or librational) modes of the nitrate ion while those above 100  $\text{cm}^{-1}$  are due to translational modes.<sup>19,20</sup> Considering the above, we believe all peaks observed at 180–360  $\text{cm}^{-1}$  in the far-IR spectra of  $\text{NONO}_3$  are most likely due to the vibrations between the  $\text{NO}^+$  and  $\text{NO}_3^-$  ion pair, while rotational modes may occur at lower frequencies (not resolved in the present study). This assignment is based on the assumption that  $\text{NO}^+$  is similar to  $\text{K}^+$  as a rigid and fully charged ion (with a molar mass between  $\text{Na}^+$  and  $\text{K}^+$ ), since the vibrational correlation between the  $\text{NO}^+$  group and  $\text{NO}_3^-$  will double the number of possible optical modes. Other differences could arise from differences in space group (see Ref. 10). Further x-ray and spectroscopic studies are required to address these issues.

One of the interesting questions regarding nitrosonium nitrate is the degree of ionicity, or symmetry breaking charge transfer in the material, and how this changes with pressure. Our previous work suggested evidence for an increase in

charge transfer with increasing pressure based on the behavior of the high frequency mid-IR bands.<sup>9</sup> The far-IR contains much more definitive information, in part because of some uncertainty in the assignment of the higher frequency bands, but this region was not explored in the previous study. Clearly, the overall intensity of the bands in the far-IR region increases with pressure, indicating that the ionicity of  $\text{NO}^+\text{NO}_3^-$  is enhanced by pressure. An empirical estimate of the ionicity can be obtained from the classical damped oscillator model, in terms of the dynamic effective charge associated with a particular vibrational mode. The dynamic effective charges give a measure of the static charges in the system. The model expresses the electronic polarization of a molecule as<sup>21</sup>

$$\epsilon - n^2 = \left(\frac{n^2 + 2}{3}\right)^2 N \frac{(sz e)^2}{\pi m \nu_i^2}, \quad (2)$$

where  $\epsilon$  is the static dielectric constant,  $n$  the optical refractive index,  $\nu_i$  the frequency of the mode and  $m$  the reduced mass of the ion pair,  $N$  the number oscillators per unit volume,  $z$  the valency of the ions, and  $e$  the electron charge. From this, one can derive  $s$ , the reduced form of the dynamic effective charge,

$$s = \frac{\nu_i}{e} \frac{3}{n^2 + 2} \sqrt{\frac{\pi m f}{N}}, \quad (3)$$

where  $f = \epsilon - n^2$  is the oscillator strength. For example, the effective charge associated with the strong lattice mode at  $372 \text{ cm}^{-1}$  obtained using the parameters assumed previously ( $n = 1.75$ ,  $m = 20.2 \text{ g/mol}$ ,  $N = 1.9 - 2.2 \times 10^{22}/\text{cm}^3$ )<sup>9,10</sup> ranged from  $0.11e$  to  $0.17e$  in the pressure interval of 13–32 GPa. This corresponds to the observed intensity change by a factor of 2.4. The pressure dependence of IR absorption was found to be more prominent for the lattice modes than for the intramolecular modes, indicating that intermolecular electronic polarization responds more strongly to pressure than does intramolecular polarization. The value of the dynamic effective charges implies a value of the static effective charge to be less than for ionic compounds such as NaCl or KBr, whose effective charges are  $0.74e$  and  $0.76e$ , respectively (i.e., much closer to unity).<sup>21</sup>

The frequencies and pressure dependences of the mid-IR absorption bands (Fig. 2) are consistent with the previous study.<sup>9</sup> However, the relative intensities of the bands in the two studies show some variability. Indeed, these differences were found from run to run in this study with  $\text{N}_2\text{O}$  and with  $\text{N}_2\text{O}_4$  as starting materials. These differences are likely to be associated with variability in laser heating temperature in different runs, resulting in slight differences in order/disorder and the presence of ionic defects. These must be particularly IR-sensitive as the Raman profiles from different runs are virtually indistinguishable. Nevertheless, the IR data taken together provide a basis for testing assignments of the bands, which is important for fully characterizing the material and its transformations as a function of pressure and temperatures.

Two IR bands with moderate intensity at the highest frequencies (e.g.,  $2340$  and  $2439 \text{ cm}^{-1}$  at 32.5 GPa) are ob-

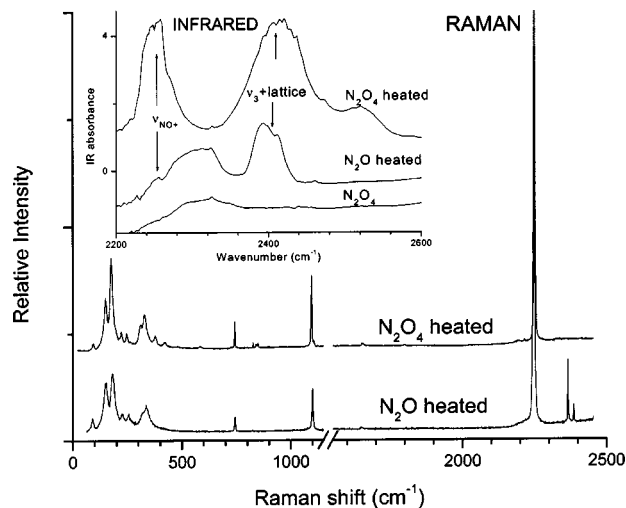


FIG. 8. Raman spectra of heated  $\text{N}_2\text{O}_4$  and  $\text{N}_2\text{O}$  near 13 GPa. The  $1150$ – $1450 \text{ cm}^{-1}$  region corresponds to the region of the strong diamond first-order Raman signal and has been omitted. The inset shows IR absorbance of heated  $\text{N}_2\text{O}_4$ , heated  $\text{N}_2\text{O}$  and pure  $\text{N}_2\text{O}_4$  measured at 13 GPa and room temperature.

served consistently at all pressures. Previous analysis of these peaks suggested that they are combination bands originating from the  $\text{NO}^+$  stretching mode ( $2265 \text{ cm}^{-1}$ ) and far-IR lattice modes (at about  $75$  and  $174 \text{ cm}^{-1}$ ).<sup>9</sup> Our measurement of the far-IR spectrum reveals a strong and broad lattice peak about  $300 \text{ cm}^{-1}$  (Fig. 1) well above the anticipated region, casting doubt on that assignment. Another explanation for these fairly strong bands would be IR-active  $\text{N}_2$  vibrons.<sup>9</sup> The IR active  $\nu_2$  mode of  $\text{N}_2$  reported by Bini *et al.*<sup>22</sup> occurs at  $2330$ – $2380 \text{ cm}^{-1}$  from 10 to 27 GPa. In addition, this mode remains a singlet below 18.3 GPa and splits into a doublet above that pressure. The two bands observed in the present study, however, appear at different frequencies (i.e.,  $2241$ – $2381 \text{ cm}^{-1}$  and  $2373$ – $2438 \text{ cm}^{-1}$ , respectively), and have much higher intensity at all pressures than those of bulk  $\text{N}_2$ .<sup>22</sup>

Spectra of  $\text{NO}^+\text{NO}_3^-$  formed by heating  $\text{N}_2\text{O}_4$  at high pressures were used to identify these peaks. Raman and IR spectra are presented in Fig. 8. Heating both  $\text{N}_2\text{O}_4$  and  $\text{N}_2\text{O}$  produces ionic  $\text{NO}^+\text{NO}_3^-$  as confirmed by almost identical Raman bands. Only minor differences are discernible, such as additional lattice features and the  $\nu_2$  multiplet at  $830 \text{ cm}^{-1}$  in the spectrum of heated  $\text{N}_2\text{O}_4$ , as well as the lack of  $\text{N}_2$  vibrons at  $2365$  and  $2386 \text{ cm}^{-1}$  observed in the spectrum of heated  $\text{N}_2\text{O}$ . The inset shows IR spectra of  $\text{N}_2\text{O}_4$  before and after heating in comparison with heated  $\text{N}_2\text{O}$ . A dramatic difference in the IR spectra of unheated and heated  $\text{N}_2\text{O}_4$  is observed: the two strong peaks at  $2250$  and  $2415 \text{ cm}^{-1}$  provide unambiguous evidence for a structural change induced by heating. The former peak is assigned to the  $\text{NO}^+$  stretching mode, consistent with previous work.<sup>9</sup> The latter could originate from the combination of  $\nu_3$ , the  $\text{NO}_3^-$  asymmetric stretching mode and the peak at  $1034 \text{ cm}^{-1}$ , which is also a combination from two lattice modes. A combination excitation associated with strong fundamentals is expected to be intense. In the IR spectrum of heated  $\text{N}_2\text{O}$ , however, the  $\text{NO}^+$  stretching mode was found weak while the combina-

tion peak appears as strong as the heated  $\text{N}_2\text{O}_4$ . Since the peak at  $2310\text{ cm}^{-1}$  was not observed in heated  $\text{N}_2\text{O}_4$  (i.e., pure  $\text{NO}^+\text{NO}_3^-$ ), alternatively, the band could be assigned to  $\text{N}_2$  molecules alloyed with  $\text{NO}^+\text{NO}_3^-$  (i.e., not a separate phase).<sup>9</sup> The position of this peak occurs at slightly lower frequencies than the pure  $\text{N}_2$  vibron at the same pressure ( $\sim 13\text{ GPa}$ ). If it arises from  $\text{N}_2$  trapped in  $\text{NO}^+\text{NO}_3^-$ , the absence of the corresponding peak in the Raman spectrum indicates fairly low concentrations, hence the intrinsic cross section (polarization) would have to be very high. A satisfactory interpretation of this mode requires further experimental and theoretical investigation.

Between 32 and 10 GPa, the IR bands in both the lattice mode and internal vibration regions evolve smoothly with pressure. The pressure dependence of the major IR-active modes is close to linear, and fairly gradual. For instance, the lattice mode at  $372\text{ cm}^{-1}$  exhibits a pressure shift of  $5.33\text{ cm}^{-1}/\text{GPa}$ , whereas the  $\nu_4$ ,  $\nu_2$ ,  $\nu_1$  internal vibrational modes of  $\text{NO}_3^-$  have  $(d\nu/dP)_T = 1.40$ ,  $0.46$ , and  $2.65\text{ cm}^{-1}/\text{GPa}$  for  $\nu_4$ ,  $\nu_2$ , and  $\nu_1$ , respectively. The smooth evolution of the major IR modes indicates a single phase of  $\text{NO}^+\text{NO}_3^-$  persists in this broad pressure region, consistent with x-ray diffraction measurements.<sup>10</sup> However, when the pressure is reduced further, a significant change in the absorption is observed. For example, at about 3 GPa, the IR spectrum exhibits a significant redshift of the lattice mode, accompanied by abundant new IR bands at  $600\text{--}800\text{ cm}^{-1}$ , and the disappearance of the peak at  $1800\text{ cm}^{-1}$ , although the major internal modes ( $\nu_4$ ,  $\nu_2$ , and  $\nu_1$ ) are preserved (Fig. 2). These changes strongly suggest that a new phase of  $\text{NO}^+\text{NO}_3^-$  occurs in the low-pressure region. On further release of pressure to below 1 GPa (Fig. 2), the absorption pattern again changed dramatically, including the loss of characteristic modes of ionic  $\text{NO}^+\text{NO}_3^-$ . We conclude that below 1 GPa,  $\text{NO}^+\text{NO}_3^-$  has transformed to molecular  $\text{N}_2\text{O}_4$ , since the major peaks match the active modes of  $\text{N}_2\text{O}_4$  unambiguously.<sup>13–16,23</sup> The three strongest peaks centered at  $740$ ,  $1250$ , and  $1722\text{ cm}^{-1}$  can be assigned (Fig. 2 and Table I) as  $\nu_{12}$  ( $B_{3u}$ ,  $\text{NO}_2$  deformation),  $\nu_{11}$  ( $B_{3u}$ ,  $\text{NO}_2$  symmetric stretch) and  $\nu_9$  ( $B_{2u}$ ,  $\text{NO}_2$  asymmetric stretch) of ordered or disordered  $\text{N}_2\text{O}_4$ .<sup>13–16,19</sup>

The characteristic absorption peaks observed in the present study, such as  $\nu_{\text{NO}^+}$  ( $2264\text{ cm}^{-1}$ ),  $\nu_1$  ( $1130\text{ cm}^{-1}$ ,  $\text{NO}_3^-$  symmetric stretch) and  $\nu_3$  ( $1403\text{ cm}^{-1}$ ,  $\text{NO}_3^-$  asymmetric stretch), are in excellent accord with the previous IR investigations of  $\text{NO}^+\text{NO}_3^-$  conducted at atmospheric pressure and at low temperatures.<sup>13–16</sup> However, we observed additional peaks in both low and high frequency IR spectra that were not observed in the previous atmospheric pressure measurements. As an ionic form of molecular  $\text{N}_2\text{O}_4$ , nitrosonium nitrate had previously been produced by thermal or photolytic autoionization.<sup>3–6</sup> The  $\text{N}_2\text{O}_4$  molecule is planar with  $D_{2h}$  symmetry but has an unstable, asymmetric isomer  $\text{ONO}-\text{NO}_2$  (denoted  $D''$  in Ref. 6) which is believed to be the precursor of  $\text{NO}^+\text{NO}_3^-$ . However, Givan *et al.*<sup>16</sup> reported observing a direct transformation of  $\text{N}_2\text{O}_4$  to  $\text{NO}^+\text{NO}_3^-$  at atmospheric pressure without precursors or subsequent induction by visible light. Therefore, the nature of this conversion process, speculated as arising from either

intra- or intermolecular mechanisms, still poses an interesting question.

The transformation between molecular  $\text{N}_2\text{O}_4$  and ionic  $\text{NO}^+\text{NO}_3^-$  has been investigated since the early 1980s. Bolduan *et al.*<sup>6</sup> reported observing temperature-induced autoionization of solid  $\text{N}_2\text{O}_4$  condensed on the surface of a copper mirror. They discovered that when the  $\text{N}_2\text{O}_4$  was heated to 180 K, autoionization to ionic  $\text{NO}^+\text{NO}_3^-$  occurs and the product remains stable from 15 to 180 K. The transformation temperature in our experiments, which is between 180 and 190 K, is in excellent agreement with their result. However, our experiments correspond to the opposite transformation, from ionic  $\text{NO}^+\text{NO}_3^-$  to molecular  $\text{N}_2\text{O}_4$ . The combination of results of the present study with previous observations<sup>6</sup> provides convincing information about the thermodynamic properties of ionic  $\text{NO}^+\text{NO}_3^-$  and molecular  $\text{N}_2\text{O}_4$ , specifically that (1)  $\text{NO}^+\text{NO}_3^-$  is the more stable phase at low temperatures and ambient pressure; (2) the transformation from either side involves a thermochemical barrier characterized by a temperature of about 180 K at ambient pressure; and (3) the transformation is reversible.

For the Raman profile of the internal mode region (e.g.,  $\nu_4$ ,  $\nu_1$  and  $\nu_{\text{NO}^+}$ ), we find good agreement between the present study and previous work on  $\text{NO}^+\text{NO}_3^-$ . However, significant differences appear in the lattice mode region between the material formed from  $\text{N}_2\text{O}$  and from  $\text{N}_2\text{O}_4$  in our work and previous reports. In previous Raman studies of the transformation of  $\text{N}_2\text{O}_4$  to  $\text{NO}^+\text{NO}_3^-$ , only two weak peaks centered at  $60$  and  $125\text{ cm}^{-1}$  were observed.<sup>3</sup> In contrast, we found a total of eight clearly resolved peaks below  $360\text{ cm}^{-1}$ , despite the fact that both studies examined the material at almost identical  $P$ – $T$  conditions (ambient pressure and 80 K). This difference suggests that the detailed structure, or the degree of order/disorder of  $\text{NO}^+\text{NO}_3^-$  formed by high pressure  $\text{N}_2\text{O}$  differs from that formed by autoionization of  $\text{N}_2\text{O}_4$  at atmospheric pressure or under pressure. We conclude that instead of amorphous  $\text{NO}^+\text{NO}_3^-$  produced by autoionization of different forms of  $\text{N}_2\text{O}_4$ , laser heating of  $\text{N}_2\text{O}$  results in the formation of ordered or crystalline  $\text{NO}^+\text{NO}_3^-$  at high pressure, and this ordered structure remains stable and can be recovered at ambient pressure and low temperature (80 K).

The ordered or crystalline structure of the  $\text{NO}^+\text{NO}_3^-$  phase documented in the present study is also consistent with the observation of a pressure-induced reversible transformation between the molecular and ionic forms reported by Angew *et al.*<sup>8</sup> In their Raman measurement of  $\text{NO}^+\text{NO}_3^-$  at room temperature, two sharp and intense peaks occur in the lattice region at 3.1 GPa, consistent with crystalline material. They suggest that this ionic form of  $\text{NO}^+\text{NO}_3^-$  is the thermodynamically favored structure at high density. Our x-ray diffraction investigation supports this argument.<sup>10</sup>

Our Raman measurements at both room and low temperature establish that crystalline  $\text{NO}^+\text{NO}_3^-$  is favored either by high pressure or low temperature or both. In addition, both the pressure-induced and temperature-induced transformation of  $\text{NO}^+\text{NO}_3^-$  to molecular  $\text{N}_2\text{O}_4$  may proceed via amorphous  $\text{NO}^+\text{NO}_3^-$  as a precursor. This is evident from comparison of the Raman spectrum of  $\text{NO}^+\text{NO}_3^-$  at 0.8



and 1.0 GPa and room temperature (Fig. 3) with that at ambient pressure and 190 K [Fig. 7(a)]. These spectra represent the Raman response measured at threshold pressures of the transformation from  $\text{NO}^+\text{NO}_3^-$  to  $\text{N}_2\text{O}_4$ , in which the lattice region displays weak and broadened peaks that could be associated with amorphous  $\text{NO}^+\text{NO}_3^-$ .

## V. CONCLUSIONS

Detailed studies indicate a broad range of stability of  $\text{NO}^+\text{NO}_3^-$  formed under a variety of conditions and from different starting materials. Far- and mid-IR measurements of the ionic isomer  $\text{NO}^+\text{NO}_3^-$  up to 32 GP revealed the major IR-active lattice modes and intramolecular vibrational modes as well as their combinations, and the IR pressure dependences.  $\text{NO}^+\text{NO}_3^-$  forms a crystalline phase at high pressure. Moreover, it is quenchable to ambient pressure and low temperature. Our Raman measurements conducted at various temperatures agree with previous studies of the transformation of  $\text{N}_2\text{O}_4$  to  $\text{NO}^+\text{NO}_3^-$ . The low temperature measurements provide evidence of a phase transition near 5 GPa. There are differences in the Raman and IR spectra of  $\text{NO}^+\text{NO}_3^-$  formed from  $\text{N}_2\text{O}$  by laser heating and from  $\text{N}_2\text{O}_4$  autoionization either at ambient pressure and low temperatures or under pressure. These differences can be attributed to different degrees of order/disorder in that material.

## ACKNOWLEDGMENTS

This work was supported by Lawrence Livermore National Laboratory (Subcontract No. B525927 to Harvard University), by AFOSR and DARPA (F-49620-02-1-01859) and by NSF. We are grateful to A. F. Goncharov for assistance with the Raman measurements, to O. Tschauner for

laser heating, and to V. V. Struzhkin, J. J. Dong, P. F. McMillan, and A. Madduri for helpful discussions.

- <sup>1</sup>R. J. Hemley, *Annu. Rev. Phys. Chem.* **51**, 763 (2000).
- <sup>2</sup>D. R. Herschbach, *Annu. Rev. Phys. Chem.* **51**, 1 (2000).
- <sup>3</sup>S. F. Agnew, B. I. Swanson, L. H. Jones, and R. L. Mills, *J. Phys. Chem.* **89**, 1678 (1985).
- <sup>4</sup>L. Parts and J. T. Miller, *J. Chem. Phys.* **43**, 136 (1965).
- <sup>5</sup>F. Bolduan and H. J. Jodl, *Chem. Phys. Lett.* **85**, 283 (1982).
- <sup>6</sup>F. Bolduan, H. J. Jodl, and A. Loewenschuss, *J. Chem. Phys.* **80**, 1739 (1984).
- <sup>7</sup>L. H. Jones, B. I. Swanson, and S. F. Agnew, *J. Chem. Phys.* **82**, 4389 (1985).
- <sup>8</sup>S. F. Agnew, B. I. Swanson, L. H. Jones, R. L. Mills, and D. Schiferl, *J. Chem. Phys.* **87**, 5065 (1983).
- <sup>9</sup>M. Somayazulu, A. F. Goncharov, O. Tschauner, P. F. McMillan, H. K. Mao, and R. J. Hemley, *Phys. Rev. Lett.* **87**, 135504 (2001).
- <sup>10</sup>Y. Song, M. Somayazulu, H. K. Mao, R. J. Hemley, and D. R. Herschbach, *J. Chem. Phys.* **118**, 8330 (2003).
- <sup>11</sup>H. K. Mao, J. Xu, and P. M. Bell, *J. Geophys. Res., [Space Phys.]* **91**, 4673 (1986).
- <sup>12</sup>A. F. Goncharov, V. V. Struzhkin, R. J. Hemley, H. K. Mao, and Z. Liu, *Science and Technology of High Pressure*, edited by M. H. Manghnani, W. Nellis, and M. Nicol (Universities Press, Hyderabad, India, 1, 1999), p. 90.
- <sup>13</sup>A. Givan and A. Loewenschuss, *J. Chem. Phys.* **90**, 6135 (1989).
- <sup>14</sup>A. Givan and A. Loewenschuss, *J. Chem. Phys.* **91**, 5126 (1989).
- <sup>15</sup>A. Givan and A. Loewenschuss, *J. Chem. Phys.* **93**, 7592 (1990).
- <sup>16</sup>A. Givan and A. Loewenschuss, *J. Chem. Phys.* **94**, 7562 (1991).
- <sup>17</sup>G. Turrell, *Infrared and Raman Spectra of Crystals* (Academic, London, 1972), see p. 107.
- <sup>18</sup>W.-J. Lo, M.-Y. Shen, C.-H. Yu, and Y.-P. Lee, *J. Mol. Spectrosc.* **183**, 119 (1997).
- <sup>19</sup>M. Balkanski, M. K. Teng, and M. Nusimovici, *Phys. Rev.* **176**, 1098 (1968).
- <sup>20</sup>D. Liu, F. G. Ullman, and J. R. Hardy, *Phys. Rev. B* **45**, 2142 (1992).
- <sup>21</sup>B. Szigetti, *Proc. R. Soc. London, Ser. A* **204**, 51 (1950).
- <sup>22</sup>R. Bini, L. Ulivi, J. Kreutz, and H. J. Jodl, *J. Chem. Phys.* **112**, 8522 (2000).
- <sup>23</sup>C. H. Bibart and G. E. Ewing, *J. Chem. Phys.* **61**, 1284 (1974).